STATIONARY AND NONSTATIONARY NONLINEAR SPECTROSCOPY OF GaSe

V.M. PETNIKOVA, M.A. KHARCHENKO and V.V. SHUVALOV
Department of Physics, Moscow State University, Lenin's Hills, Moscow 119 899, USSR

Received 15 September 1987; accepted for publication 22 September 1987
Communicated by V.M. Agranovich

An effective complex investigation of semiconductors by means of nonlinear spectroscopy is reported. The main nonlinearity physical mechanisms are investigated and characteristic times of some relaxation processes are measured in GaSe at 293 K.

1. Semiconductors and, in particular, GaSe are complicated objects for spectroscopic investigations, because:

(1) their response is formed by a number of nonlinear mechanisms;

(2) they are characterized by their own types of relaxation processes with corresponding times;

(3) there is no general theory to explain results obtained by different methods under different conditions;

(4) experimental data are affected simultaneously by a number of hardly controlled factors (dependence of sample transmission on wave intensities, frequencies, etc.).

Relaxation process times are measured by comparison of experimental data with theoretical models [1–5]. Therefore, the choice of the model determines the author's conclusions. Experimentalists usually use the simplest models of some selected (sometimes incorrect) relaxation processes. The creation of a complete theory is difficult due to the fact that the available experimental material is, actually, a number of data obtained in different, seldom strictly described conditions. Physical processes occurring in semiconductors can be understood with the help of the maximum possible number of spectroscopic methods applied under the same conditions. Complex analysis of all these research results can provide new information unaccessible to each single method about relaxation process mechanisms.

The necessity of such complex investigations has been proved and a way of its realization has been suggested [6]. In these experiments two frequency-tunable radiation sources were used. Their pulses had intermediate duration between two characteristic groups of fast ($\leqslant 1$ ps) and slow ($\geqslant 100$ ps) relaxation times in semiconductors. The fast processes (for example polarization relaxation) were investigated by spectral analysis methods (biharmonic pumping, BP), and the slow, nano- and subnanoseconds (interband transitions, spatial diffusion of carriers, etc.) by analysis in the time domain (probe pulse method, pp). Such an approach coupled with polarization techniques gave the opportunity to identify some types of relaxation processes and to measure their times.

2. This Letter presents an analysis of the experimental results of temporal and frequency cubic nonlinear susceptibility dispersion in the GaSe one-photon interband and exciton transition region. Potential possibilities and complete usage of the experimental setup [6] permitted us to realize the complex of such nonlinear spectroscopy (NS) methods as BP, PP, saturation spectroscopy (SS), and degenerate four-photon spectroscopy (DFPS).

These NS methods are based on the generation of a nonlinear polarization wave with wave vector $\boldsymbol{K}_4=\boldsymbol{K}_l-\boldsymbol{K}_m+\boldsymbol{K}_n$ and frequency $\omega_4=\omega_l-\omega_m+\omega_n$ ($l, m, n=1, 2, 3$), which also lies in the innvestigated region. In accordance with the NS method the concrete polarization wave spatial component (appro-

0375-9601/87/$ 03.50

Table 1
NS methods.

NS method ref.	$K_4=$	Main variable	Varied parameters	Measured quantity	Fig.
SS [1]	$K_1-K_1+K_1$	pulse intensities	freqency	transmission spectrum $T(\nu_4)$.	2,3
	$K_1-K_2+K_2$		frequencies, polarizations	T deviation	
PP [1–3,6]	$K_1-K_2+K_2$	pulse time delay	frequency detuning, polarizations of waves	T deviation	2,3,5
	$K_1-K_2+K_3$			diffraction efficiency	4
DFPS [4]	$2K_1-K_2$	pulse frequencies	polarizations of waves	selfdiffraction efficiency (SD)	6
BP [5,6]	$2K_1-K_2$	frequency detuning	central frequency	SD efficiency	7,8

priate direction of K_4) is registrated. Automatized experimental setup had proved independent control of time delays, polarizations, frequencies, intensities of interacting pulses. The NS methods are shown in table 1.

3. The compute controlled expeimental setup block diagram is shown in fig. 1. In general it does not differ from the setup described in ref. [6]. The presence of GaSe excellent cleavage planes, which are orthogonal to its optical axis, permitted us to obtain perfect optical quality oriented samples of 10–30 μm thickness. The spectral-limited picosecond (of 25 ps duration, 100 kW peak power) and nanosecond (of 10 MHz bandwidth, 1 kW peak power) pulses of dye lasers tuned in the 605–645 nm range were used. The tuning region overlapped the ranges of transparency, one-photon exciton and interband transitions of the GaSe sample. The frequency coincidence was fixed by the presence of a stable inteference pattern of two independent laser beams. The main features of the modificated experimental setup used were:

(1) application of organic dye 2681 in polymer matrix [7] for picosecond Nd:YAG mode-locking (stabel laser generation during 2 years of setup operation, 3 million generation cycles);

(2) application of LiF crystal with F_2^- colour centres in the decoupling system (98% mode-locking probability with 5–6% train energy dispersion);

(3) an increased number of computer controlled monitoring system channels (allowing for absorption saturation in DFPS and BP methods etc.);

(4) usage of frequency tuning spectral-limited nanosecond pulses for subnanosecond relaxation process investigations by high-resolution spectral analysis methods (BN and DFPS).

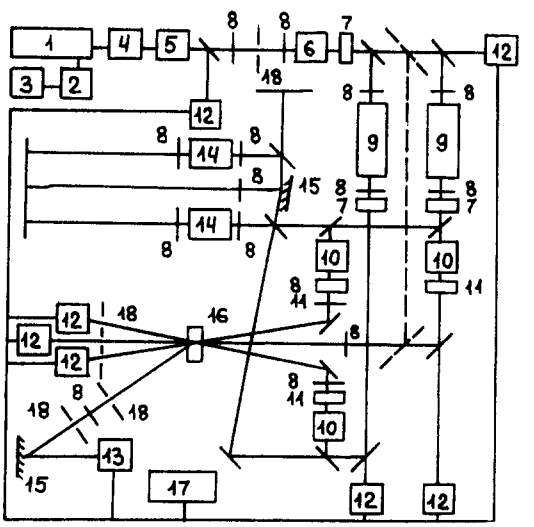

Fig. 1. Experimental setup: (1) master oscillator; (2) high-speed photodiode; (3) high-speed oscilloscope; (4) decoupling system; (5) amplifier; (6) frequency doubler; (7) filters; (8) lenses; (9) dye-lasers; (10) delay lines; (11) polarization control system; (12) energy detectors; (13) photomultiplier; (14) Fabry–Perot etalons; (15) diffraction gratings; (16) sample; (17) computer; (18) diaphragms.

The experimental setup provides the necessary degrees of freedom for realization of all above NS methods.

4. In the SS method the probe pulse transmission spectrum $T(\lambda_1)$ (fig. 2) and its relative deviation $\delta T(\lambda_1)$ (fig. 3) under pump pulse intensity I_2, polarization (with respect to probe) and frequency ($\lambda_2 = 609$, 617.5 nm) variations, has been investigated. Under 20 kW peak power, ~ 20 μm sample thickness and 0.2–0.5 mm excitation region diameter it is possible to estimate the electron–hole pair concentration n as $\gtrsim 10^{16}$ cm^{-3}. The SS method evolves into the absorption variant of the PP one when the time delay between interacting pulses was introduced (figs. 2 and 3). In the PP method the efficiency of diffraction on transient gratings, formed by simultaneously acting pump pulses, via probe pulse time delay was measured (fig. 4). The acting wave frequency detuning Δ and the relative orientation of the polarization vector were varied. The probe pulse transmission dynamics determined the dynamics of the carrier population relaxation $n(\tau)$ under the same experimental conditions (fig. 5).

In the DFPS method the SD efficiency η was measured via the wave lengths of the interacting beams $\lambda_1 = \lambda_2 = \lambda_3 = \lambda$ (fig. 6) under orthogonal and parallel polarizations of the pumps. The nonlinear

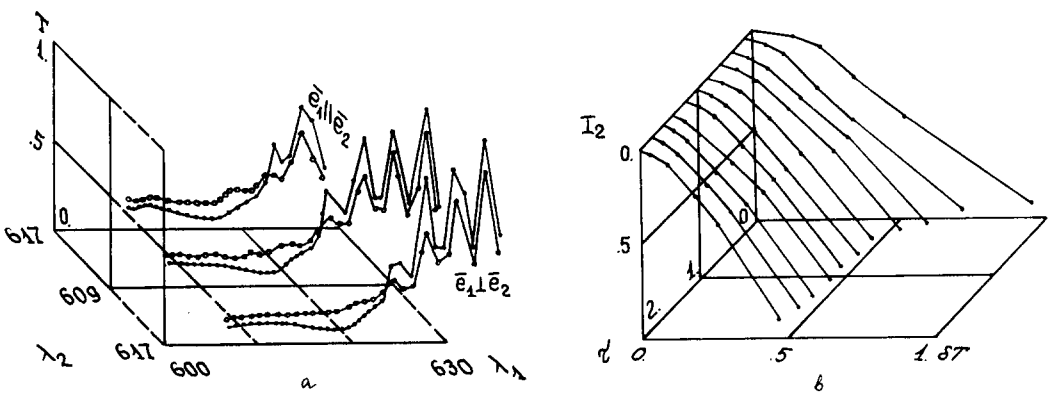

Fig. 2. SS method, absorption variant of PP method: (a) transmission spectrum $I(\lambda_1)$, $I_2 = 0$ (·), $I_2 \neq 0$ (○); (b) deviation of transmission $\delta T(I_2)$. $\lambda_2 = 617.5$ nm, $e_1 \| e_2$.

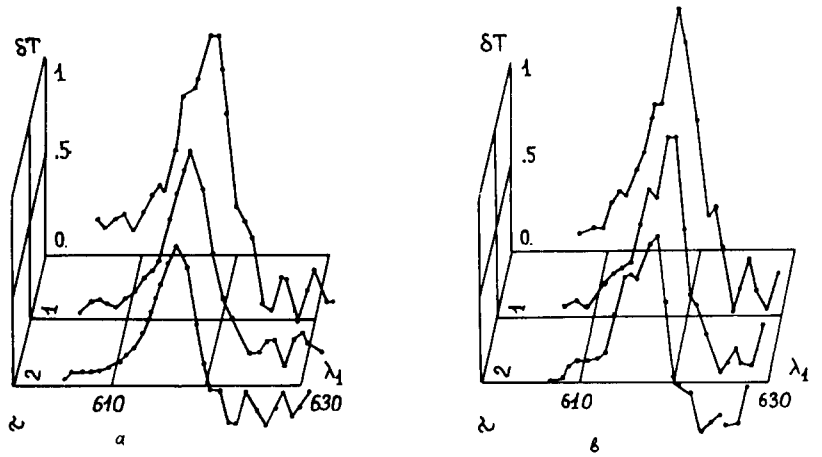

Fig. 3. SS method, absorption variant of PP method: deviation of transmission $\delta T(\lambda_1)$, $e_1 \| e_2$; (a) $\lambda_2 = 609$ nm, (b) 617.5 nm.

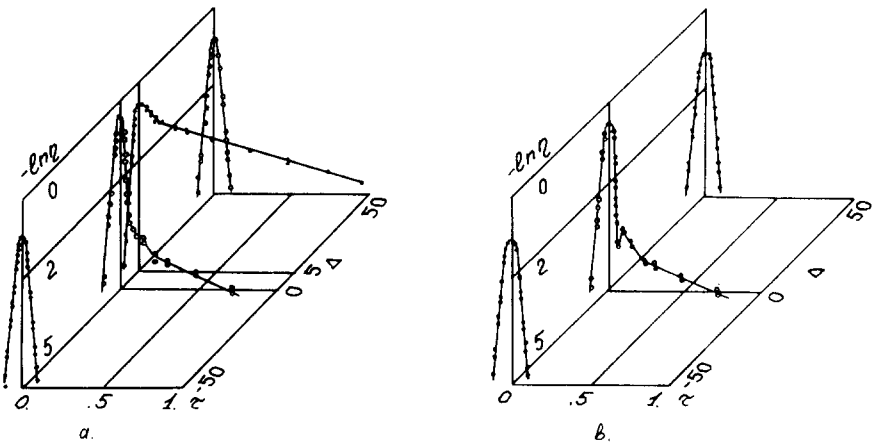

Fig. 4. PP method: transient gratings diffraction efficiency $\eta(\tau)$: (a) $e_1 \parallel e_2$, (b) $e_1 \perp e_2$.

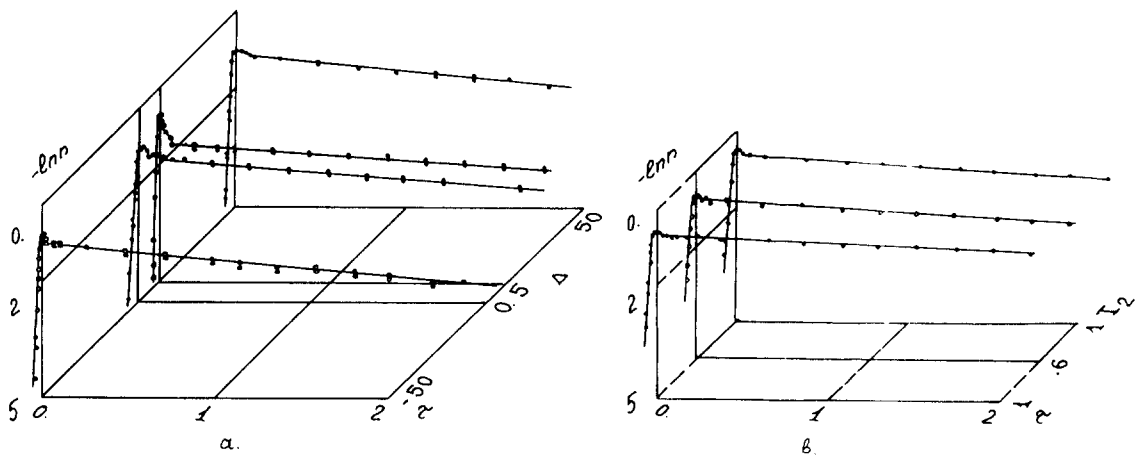

Fig. 5. Absorption variant of PP method: dynamics of population $n(\tau)$; $\lambda = 617.5$ nm, $e_1 \parallel e_2$, variation of (a) Δ and (b) I_2.

susceptibility modulus squared $|\chi|^2$ was calculated with the help of the sample transmission coefficient measured simultaneously. In some experiments additional illumination by Nd:YAG laser second harmonic pulses with peak intensity I was used (fig. 6).

In the BP method the SD efficiency η via frequency detuning $\Delta = \omega_1 - \omega_2$ (fig. 7) and $\Delta = \omega_2 - \omega_1$ (fig. 8) was measured. The central frequency – frequency coincidence point in GaSe absorption spectrum $\lambda_0 = 620.4$ (the exciton transition wing); 617.5 (exciton resonance); 614; 609 nm (interband transitions) – was varied. The orthogonal pump wave polarizations $e_1 \perp e_2$) were chosen to eliminate scattering on sound gratings [6].

5. A complete analysis of all experimental results enables us to draw the following conclusions.

(1) In the frequency region investigated the GaSe nonlinear response is formed by exciton, electron and polariton mechanisms. The corresponding transition characteristic frequencies were identified. The peaks of the transmission coefficient deviation δT (SS, fig. 3) and nonlinear susceptibility of SD process η under parallel pump pulse polarizations (DFPS, fig. 6)

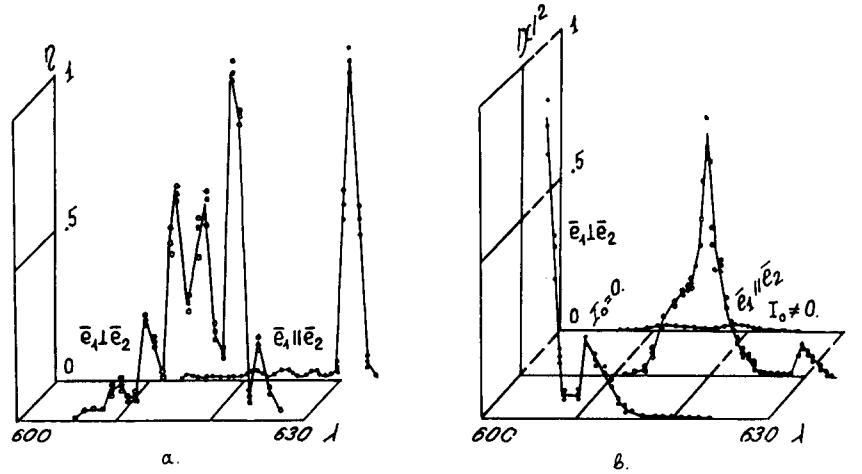

Fig. 6. DFPS method: (a) self-diffraction efficiency $\eta(\lambda)$ and (b) nonlinear susceptibility $|\chi|^2(\lambda)$.

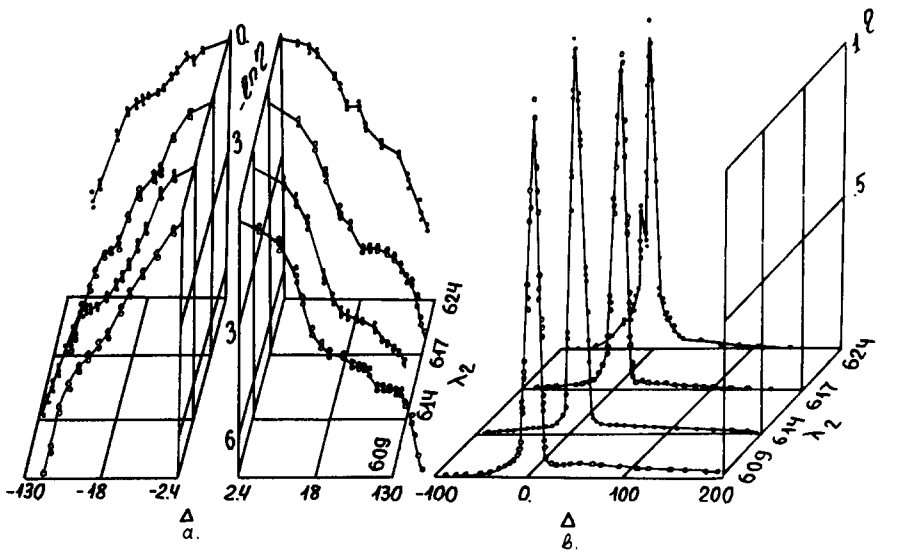

Fig. 7. BP method: self-diffraction efficiency $\eta(\Delta)$, tuning of λ_1, (a) logarithmic and (b) linear scale.

lie near the exciton resonance. The DFPS under orthogonal polarizations showed a significant increase as the frequency was tuned to the interband transition region (fig. 6). In the GaSe transparency region subordinate peaks of the SD process efficiency η were observed (BP, fig. 8). Their frequency positions practically exactly corresponded to the well-known LO and TO phonon frequencies [8]. Exciton absorption line saturation (SS, fig. 2), exciton screening by free carriers (DFPS with illumination by Nd:YAG laser second harmonic pulses, fig. 6), and band renormalisation (SS and PP absorption variant, figs. 2 and 3) were observed.

(2) Under our experimental conditions several types of relaxation processes played a main role.

The subpicosecond polarization relaxation dynamics was determined by electron–phonon interaction. It was displayed most clearly in BP

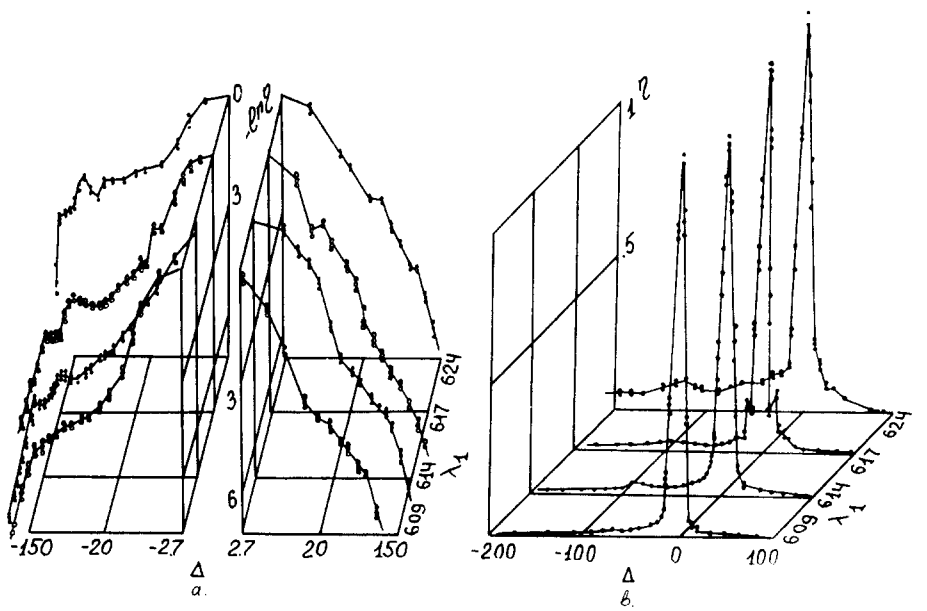

Fig. 8. BP method: self-diffraction efficiency $\eta(\Delta)$, tuning of λ_0. (a) logarithmic and (b) linear scale.

experiments (figs. 7 and 8). The central symmetrical peak of the SD process efficiency η is connected with low frequency phonons. The interaction with high frequency phonons, not excited at equilibrium, broadens the Stokes wing of $\eta(\Delta)$. Under tuning to the interband transition region the polariton subordinate peaks are smoothing, and at $\lambda_0 = 609$ nm (figs. 7 and 8) the blue wing of $\eta(\Delta)$ may be approximated by the lorentzian function $(1+\Delta^2/\gamma^2)^{-2}$. The effective width $\gamma = 150 \pm 20$ cm^{-1} corresponds to a transverse relaxation time $T_2 = \gamma^{-1} = 36 \pm 5$ fs (two-level model) But the asymmetry of the dispersion curve points out the inapplicability of such model-polarization; the dynamics may be more complicated, in particular, bi-exponential.

Picosecond transient grating decay dynamics $\leqslant 420+20$ ps is due to spatial diffusion of carriers. It was registrated by methods of PP with picosecond light sources (fig. 4) and BP with nanosecond pulses.

Nanosecond relaxation dynamics of population n with characteristic time 5 ± 2 ns was registrated by the absorption variant of PP (fig. 5).

(3) Under excitation of electron (exciton) transitions in the semiconductor the phonon subsystem, as vibrational one in molecular media, is effectively excited by BP (figs. 7 and 8) or subpicosecond pulses spectral components in PP, SS, DFPS and cannot be described as a markovian bath. Polarization decay must be described by dynamical models taking into account the electron–phonon interaction coherence.

6. Usage of the complex of NS methods under the same conditions enables us to draw significantly more general physical conclusions. So, BP central frequency passage through exciton resonance did not show any features in the $\eta(\Delta)$ behaviour (figs. 7 and 8). Comparison of these results with the ones obtained by the DFPS method (fig. 6), permit us to draw the conclusion that under orthogonal polarizations the exciton nonlinearity is significantly less than that of the electron.

The data obtained may be the basis to a theoretical model of the nonlinear susceptibility of semiconductors taking into account the main physical processes and explaining all experimental results with a limited number of adjustment parameters.

References

[1] J.L. Oudar et al., J. Lumin. 30 (1985) 340;
J.L. Oudar and A. Migus, Phys. Rev. Lett. 53 (1984) 384.

[2] T.F. Bogges, A.L. Smirl and B.S. Wherett, IEEE J. Quantum Electron. 19 (1983) 680, 690.
[3] L. Schultheis, J. Kuhl, A. Honold and C.W. Tu, Phys. Rev. Lett. 57 (1986) 1635, 1797.
[4] P.P. Paskov et al., Solid State Commun. 59 (1986) 491.
[5] S.Y. Yen and P.A. Wolf, Appl. Phys. Lett. 40 (1982) 457; S.Y. Yen, Appl. Phys. Lett. 41 (1982) 590.
[6] V.M. Petnikova, S.A. Pleshanov and V.V. Shuvalov, Sov. Phys. JETP 61 (1985) 211; Opt. Spectrosk. 60 (1986) 998.
[7] M.I. Demchuk, V.P. Mihailov and A.M. Prohorov, Pisma Zh. Eksp. Teor. Fiz. 10 (1984) 338.
[8] L. Jaudl, J.L. Brebner and B.M. Powel, Phys. Rev. B 13 (1976) 686.
[9] V.M. Petnikova, S.A. Pleshanov and V.V. Shuvalov, Opt. Spektrosk. 59 (1985) 288.